On the Downlink Performance of UAV Communications in Dense Cellular Networks

David López-Pérez[1], Ming Ding[2], Huazhou Li[3], Lorenzo Galati Giordano[1],
Giovanni Geraci[1], Adrian Garcia-Rodriguez[1], Zihuai Lin[3], Mahbub Hassan[4]
[1]*Nokia Bell Labs, Ireland* {david.lopez-perez@nokia.com}
[2]*Data61, Australia*{Ming.Ding@data61.csiro.au}
[3]*University of Sydney, Australia*{huazhou.li@sydney.edu.au}
[4]*University of New South Wales, Australia*{mahbub.hassan@unsw.edu.au}

***Abstract*—A reliable command and control communication channel to unmanned aerial vehicles (UAVs) is needed to allow beyond visual line of sight (LoS) operations. Cellular networks, with their almost ubiquitous coverage, are an obvious candidate to provide it. However, up to which extent the current networks designed for ground users can support UAV communications is an open question. In this paper, we provide a comprehensive theoretical analysis, using stochastic geometry, of the performance that operators could expect from traditional cellular networks with omnidirectional antennas when supporting UAV downlink command and control channels. Our study employs the latest UAV height-dependent path loss model defined by the 3GPP, with LoS and non-LoS transmissions and a probabilistic model to switch between them. We derive analytical expressions for the coverage probability and area spectral efficiency, while accounting for base stations with idle mode capabilities, a practical finite UAV density, and different UAV heights. Results show that networks based on base stations with omnidirectional coverage can support low height UAVs but will struggle with high height ones. Densification helps to provide a better performance.**

I. Introduction

During the last century, we have seen a number of new technologies emerge, which have completely changed the way we understand our world. For example, the invention of the car in 1886, the television in 1927, and the mobile phone in 1973 transformed the way in which we humans move around, entertain ourselves, and finally communicate with each other. Yet, we are at the dawn of a new era, the era of the unmanned aerial vehicles (UAVs), also known as drones [1].

UAVs are populating the sky at a very fast pace, and new use cases appear every day. In particular, commercial UAV applications include surveillance, search and rescue, monitoring of critical infrastructures, package delivery, wildlife and nature conservation, just to name a few. Moreover, it is predicted that a rapid and vast growth in the UAV industry will bring new promising business opportunities, opening new and attractive vertical markets, which are even hard to anticipate now [2–4].

As any other new market, however, the UAV one, still in its infancy, is not free of challenges. Currently, regulations in most countries only allow for operating UAVs when there is a visual line of sight (VLoS) between the UAV pilot and the UAV itself. This regulation significantly restricts most appealing commercial UAV use cases, and thus threatens the development of the entire ecosystem [5].

In this light, there has been an increasing interest in providing a reliable command and control communication channel to UAVs, which can allow beyond visual line of sight (BVLoS) operations. In the downlink (DL), i.e., from the base station (BS) to the UAV, this control channel should allow the UAV flight control system to change the UAV trajectory to avoid potential collisions, enable dynamic geofencing, or command a range of sensor/actuator functions on board of the UAV. In the uplink (UL), i.e., from the UAV to the BS, it can be used to update the UAV flight control system with status messages and sensor information.

The key question now is how this control channel should be provided in a reliable manner. Cellular networks, having almost ubiquitous coverage, are an obvious candidate for it, in particular, LTE-based systems, as they can provide quality of service with an infrastructure that is already in place [5–10]. The cellular community, through the third generation partnership project (3GPP), has already started to consider this appealing UAV business, and is looking at providing answers to the various regulation committees, which are already specifying the rules UAV operations must conform to for BVLoS [11].

However, and here the caveat, LTE networks were not designed for aerial coverage, but optimised to serve ground user equipment (GUE). Because of this, terrestrial cellular networks present severe interference limitations when serving UAVs. Once UAVs are flying well above the BS antenna heights, they receive signals originating from many more BSs, i.e., they suffer from many more potential interferers. Moreover, these interfering signals are likely to be in line-of-sight (LoS), which further aggravates their negative impact [12–14]. As a result:

- BSs communicating with their ground UEs or UAVs in DL could create significant interference to the aerial DL transmissions of UAVs associated to neighbouring BSs (serving BSs-UAVs). See Fig. 1 for details.
- UAVs transmitting UL information to their serving BSs could create significant interference to a large number of neighbouring BSs receiving both ground UL transmissions (ground UEs-serving BSs) as well as aerial UL ones

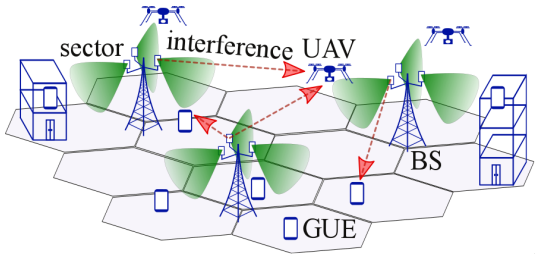

Fig. 1. DL interference from neighbouring BSs to the control and command channel of a UAV.

from other UAVs.

All these factors pose a fundamental question: *Up to which extent can current LTE and future 5G networks support UAV communications?*

To answer such question, we consider a large-scale, randomly-deployed cellular network that supports UAVs, and pay special attention to the performance of the DL channel, where the critical commands and the control channels are provided.

The main contributions of this paper are as follows:

- We perform for the first time a theoretical analysis of the DL channel performance as a function of the BS density, using stochastic geometry and the comprehensive path loss model used by the 3GPP in [11] with a probabilistic transition between LoS and NLoS conditions that accounts for the UAV height.
- We derive analytical expressions for the coverage probability and area spectral efficiency (ASE), in a practical scenario that accounts for a finite UAV density and BSs with idle mode capabilities.
- We provide a comprehensive explanation of the results, building on three known phenomena: the *ASE Crawl* [15], the *ASE Crash* [16], and the *ASE Take Off* [17].

The rest of this paper is structured as follows. Section II describes the system model. Section III presents our theoretical formulation of the coverage probability and the ASE performance, while the numerical results are discussed in Section IV, with remarks shedding new light on UAV DL performance, and the suitability of cellular networks to provide the command and control communication channel. Finally, the conclusions are drawn in Section V.

II. System Model

We consider a DL cellular network with BSs deployed on a plane surface, according to a homogeneous Poisson point process (HPPP) Φ of intensity λ BSs/km^2. UEs are also Poisson distributed in the considered network with an intensity of ρ UEs/km^2, where ρ may or may not be sufficiently larger than λ, and thus there may be BSs without UEs [17].

In practice, a BS will enter an idle mode if there is no UE connected to it, which reduces the interference to neighbouring UEs as well as the energy consumption of the network. Thus, the user distribution and association strategy (UAS) determines the set of active BSs. In this paper, we assume a practical UAS as in [15–17], where each UE is connected to the BS having the maximum average received signal strength.

Based on the previous considerations and assumptions, the set of active BSs also follows an HPPP distribution $\tilde{\Phi}$ [19], the density of which is denoted by $\tilde{\lambda}$ BSs/km^2, where $\tilde{\lambda} \leq \lambda$ and $\tilde{\lambda} \leq \rho$, since one UE is served by at most one BS.From [19, 20], $\tilde{\lambda}$ can be calculated as

$$\tilde{\lambda} = \lambda \left[1 - \frac{1}{\left(1 + \frac{\rho}{q\lambda}\right)^q} \right], \tag{1}$$

where according to [20], q depends on the path loss model, and the value $q = 3.5$ have been shown to work well in practice.

In this paper, we focus on the performance of a given frequency/time resource, with at most one scheduled UE in such resource per BS, and assume, without loss of generality, as we focus on the DL, that all UEs are UAVs.

The two-dimensional (2D) distance between a BS and an UAV is denoted by r, while the BS and UAV height are denoted as h_{BS} and h_{UAV}, respectively. Moreover, the absolute antenna height difference between a BS and an UAV is denoted by L. Thus, the 3D distance between a BS and a UAV can be expressed as $w = \sqrt{r^2 + L^2}$.

Building on [15, 16], we propose a very general and practical path loss model, in which the path loss $\zeta(w)$ associated with distance w is segmented into N pieces written as

$$\zeta(w) = \begin{cases} \zeta_1(w), & \text{when } 0 \leq w \leq d_1 \\ \zeta_2(w), & \text{when } d_1 < w \leq d_2 \\ \vdots & \vdots \\ \zeta_N(w), & \text{when } w > d_{N-1} \end{cases}, \tag{2}$$

where each piece $\zeta_n(w), n \in \{1, 2, \ldots, N\}$ is modeled as

$$\zeta_n(w) = \begin{cases} \zeta_n^{\mathrm{L}}(w) = A_n^{\mathrm{L}} w^{-\alpha_n^{\mathrm{L}}}, & \text{LoS: } \mathrm{Pr}_n^{\mathrm{L}}(w) \\ \zeta_n^{\mathrm{NL}}(w) = A_n^{\mathrm{NL}} w^{-\alpha_n^{\mathrm{NL}}}, & \text{NLoS: } 1 - \mathrm{Pr}_n^{\mathrm{L}}(w) \end{cases}, \tag{3}$$

where $\zeta_n^{\mathrm{L}}(w)$ and $\zeta_n^{\mathrm{NL}}(w), n \in \{1, 2, \ldots, N\}$ are the n-th piece path loss functions for the LoS transmission and the NLoS transmission, respectively, A_n^{L} and A_n^{NL} are the path losses at a reference distance $w = 1$ for the LoS and the NLoS cases, respectively, α_n^{L} and α_n^{NL} are the path loss exponents for the LoS and the NLoS cases, respectively, and $\mathrm{Pr}_n^{\mathrm{L}}(w)$ is the n-th piece LoS probability function that a transmitter and a receiver separated by a distance w has a LoS path, which is assumed to be a monotonically decreasing function with regard to w. In practice, A_n^{L}, A_n^{NL}, α_n^{L} and α_n^{NL} are variables obtainable from field tests [11], and it is important to highlight that they are a function of the UAV height h_{UAV} [11].

Similarly, the probability of LoS, $\mathrm{Pr}_n^{\mathrm{L}}(w)$, is also stacked into a M piece-wise function as

$$\mathrm{Pr}^{\mathrm{L}}(w) = \begin{cases} \mathrm{Pr}_1^{\mathrm{L}}(w), & \text{when } 0 \leq w \leq d_1 \\ \mathrm{Pr}_2^{\mathrm{L}}(w), & \text{when } d_1 < w \leq d_2 \\ \vdots & \vdots \\ \mathrm{Pr}_M^{\mathrm{L}}(w), & \text{when } w > d_{M-1} \end{cases}. \tag{4}$$

We also assume that each BS/UAV is equipped with an isotropic antenna, and that the multi-path fading between a BS and a UAV is modelled as independently identical distributed

(i.i.d.) Rayleigh fading, i.e., an exponential random variable (RV) with unitary mean[1] [15–17, 21, 22].

III. Coverage Probability and ASE Formulation

Using a 3D stochastic geometry analysis based on the HPPP theory, we study the DL performance of our wireless network by considering the performance of a typical UAV located at the origin, o.

We first investigate the probability of coverage, $p^{\text{cov}}(\lambda, \gamma)$, i.e., the probability that the UAV's signal-to-interference-plus-noise ratio (SINR) is above a pre-designated threshold, γ,

$$p^{\text{cov}}(\lambda, \gamma) = \Pr[\text{SINR} > \gamma], \tag{5}$$

where the SINR is calculated as

$$\text{SINR} = \frac{P\zeta(w)h}{I_{\text{agg}} + N_0}, \tag{6}$$

where h is the multi-path fading channel gain, and is modelled as an exponential RV with unitary mean, P and N_0 are the transmission power of each BS and the additive white Gaussian noise (AWGN) power at each UAV, respectively, and I_{agg} is the cumulative interference given by

$$I_{\text{agg}} = \sum_{i:\, b_i \in \tilde{\Phi} \setminus b_o} P\beta_i g_i, \tag{7}$$

where b_o is the BS serving the typical UAV located at distance w from it, and b_i, β_i, and g_i are the i-th interfering BS, the path loss associated with b_i, and the multi-path fading channel gain associated with b_i, respectively. Note that in (7), only the BSs in $\tilde{\Phi} \setminus b_o$ inject effective interference into the network, where $\tilde{\Phi}$ denotes the set of the active BSs.

Based on the path loss model in (2) with 3D distances and the considered UAS, we present our main result on the coverage probability, $p^{\text{cov}}(\lambda, \gamma)$, in Theorem 1, shown in the next page.

According to [15, 23], we also investigate the ASE in bps/Hz/km^2 for a given BS density λ, which can be computed as

$$A^{\text{ASE}}(\lambda, \gamma_0) = \tilde{\lambda} \int_{\gamma_0}^{+\infty} \log_2(1+\gamma) f_{\Gamma}(\lambda, \gamma) d\gamma, \tag{17}$$

where γ_0 is the minimum working SINR of the network, and $f_{\Gamma}(\lambda, \gamma)$ is the probability density function (PDF) of the SINR observed at the typical UAV for a particular value of λ. Based on the definition of $p^{\text{cov}}(\lambda, \gamma)$ in (5), which is the complementary cumulative distribution function (CCDF) of the SINR, $f_{\Gamma}(\lambda, \gamma)$ can be expressed by

$$f_{\Gamma}(\lambda, \gamma) = \frac{\partial(1 - p^{\text{cov}}(\lambda, \gamma))}{\partial \gamma}, \tag{18}$$

where $p^{\text{cov}}(\lambda, \gamma)$ is obtained from Theorem 1.

In the following, we present three concepts that are key to understand the performance behaviour of the studied network, as a function of the BS density and the UAV height. Although originally named after the ASE, these concepts are highly related and apply to the coverage probability explanations too.

[1]A more practical Rician fading, that has been shown not to change the qualitative trends, will be considered in the journal version of this paper.

A. The ASE Crawl

A much shorter distance between a UE and its serving BS in ultra-dense networks implies high probabilities of strong LoS transmissions. Generally speaking, LoS transmissions are helpful to improve the signal power, but they aggravate interference too. Thus, the ASE will suffer from a slow growth or even a decrease when the BS density is sufficiently large, and the strongest interference paths transition from NLoS to LoS. This performance behaviour is referred to as the *ASE Crawl* [15].

B. The ASE Crash

The existence of a non-zero antenna height difference between UEs and BSs leads to a non-zero cap on the minimum distance between them, and thus a cap on the signal power strength. Although each inter-cell interference power strength is subject to the same cap, the aggregated inter-cell interference power will overwhelm the signal power in an ultra-dense network due to the sheer number of strong interferers. Thus, the ASE will suffer from a significant loss when the BS density is sufficiently large. This performance behaviour is referred to as the *ASE Crash* [16].

C. The ASE Take Off

When the number of BSs is larger than that of UEs, the surplus of BSs encourages idle mode operations to mitigate unnecessary inter-cell interference and reduce energy consumption. Consequently, the SINR performance benefits from *i)* a BS diversity gain in UEs selecting a good serving BS, and *ii)* a decreased inter-cell interference, which is bounded by the active UE density. As a result, the signal power continues increasing with the network densification, while the interference power reduces or remains at a constant level due to the idle mode capability. This performance behaviour is referred to as the *ASE Take Off* [17].

IV. Results and Discussion

In this section, we discuss our theoretical and simulation results. For a more accurate analysis, we borrow the system parameters of the path loss model in [11], where without loss of generality, $N = 1$.

$$A_n^{\text{L}} = \begin{cases} A_1^{\text{L}} = 10^{-(2.8+2\log_{10} f_c)}, & 1.5m \le h_{\text{UAV}} \le 22.5m \\ A_2^{\text{L}} = A_1^{\text{L}}, & 22.5m < h_{\text{UAV}} \le 300m \end{cases}, \tag{19}$$

$$A_n^{\text{NL}} = \begin{cases} A_1^{\text{NL}} = 10^{-1.354-2\log_{10} f_c + 0.06(h_{\text{UAV}}-1.5)}, & 1.5m \le h_{\text{UAV}} \le 22.5m \\ A_2^{\text{NL}} = 10^{1.75-2\log_{10}(40\pi f_c/3)}, & 22.5m < h_{\text{UAV}} \le 300m \end{cases}, \tag{20}$$

$$\alpha_n^{\text{L}} = \begin{cases} \alpha_1^{\text{L}} = 2.2, & 1.5m \le h_{\text{UAV}} \le 22.5m \\ \alpha_2^{\text{L}} = \alpha_1^{\text{L}}, & 22.5m < h_{\text{UAV}} \le 300m \end{cases}, \tag{21}$$

$$\alpha_n^{\text{NL}} = \begin{cases} \alpha_1^{\text{NL}} = 3.908, & 1.5m \le h_{\text{UAV}} \le 22.5m \\ \alpha_2^{\text{NL}} = (46 - 7\log_{10} h_{\text{UAV}})/10, & 22.5m < h_{\text{UAV}} \le 300m \end{cases}. \tag{22}$$

Theorem 1. *Considering the path loss model in (2) and the presented UAS, the probability of coverage $p^{\mathrm{cov}}(\lambda,\gamma)$ can be derived as*

$$p^{\mathrm{cov}}(\lambda,\gamma)=\sum_{n=1}^{max(N,M)}\left(T_n^{\mathrm{L}}+T_n^{\mathrm{NL}}\right), \tag{8}$$

where
$T_n^{\mathrm{L}}=\int_{\sqrt{d_{n-1}^2-(h_{\mathrm{UAV}}-h_{\mathrm{BS}})^2}}^{\sqrt{d_n^2-(h_{\mathrm{UAV}}-h_{\mathrm{BS}})^2}}\Pr\left[\frac{P\zeta_n^{\mathrm{L}}\left(\sqrt{r^2+(h_{\mathrm{UAV}}-h_{\mathrm{BS}})^2}\right)h}{I_{\mathrm{agg}}+N_0}>\gamma\right]f_{R,n}^{\mathrm{L}}(r)\,dr,$
and
$T_n^{\mathrm{NL}}=\int_{\sqrt{d_{n-1}^2-(h_{\mathrm{UAV}}-h_{\mathrm{BS}})^2}}^{\sqrt{d_n^2-(h_{\mathrm{UAV}}-h_{\mathrm{BS}})^2}}\Pr\left[\frac{P\zeta_n^{\mathrm{NL}}\left(\sqrt{r^2+(h_{\mathrm{UAV}}-h_{\mathrm{BS}})^2}\right)h}{I_{\mathrm{agg}}+N_0}>\gamma\right]f_{R,n}^{\mathrm{NL}}(r)\,dr,$
and d_0 and d_N are defined as $|h_{\mathrm{UAV}}$-$h_{\mathrm{BS}}|$ and $+\infty$, respectively. Moreover, $f_{R,n}^{\mathrm{L}}(r)$ and $f_{R,n}^{\mathrm{NL}}(r)$ $\left(\sqrt{d_{n-1}^2-(h_{\mathrm{UAV}}-h_{\mathrm{BS}})^2}<r\le\sqrt{d_n^2-(h_{\mathrm{UAV}}-h_{\mathrm{BS}})^2}\right)$, are represented by

$$\begin{aligned}f_{R,n}^{\mathrm{L}}(r)=\exp\left(-\int_0^{r_1}\left(1-\Pr^{\mathrm{L}}\left(\sqrt{u^2+(h_{\mathrm{UAV}}-h_{\mathrm{BS}})^2}\right)\right)2\pi u\lambda du\right)\exp\left(-\int_0^{r}\Pr^{\mathrm{L}}\left(\sqrt{u^2+(h_{\mathrm{UAV}}-h_{\mathrm{BS}})^2}\right)2\pi u\lambda du\right)\\ *\Pr_n^{\mathrm{L}}\left(\sqrt{r^2+(h_{\mathrm{UAV}}-h_{\mathrm{BS}})^2}\right)2\pi r\lambda,\end{aligned} \tag{9}$$

and

$$\begin{aligned}f_{R,n}^{\mathrm{NL}}(r)=\exp\left(-\int_0^{r_2}\Pr^{\mathrm{L}}\left(\sqrt{u^2+(h_{\mathrm{UAV}}-h_{\mathrm{BS}})^2}\right)2\pi u\lambda du\right)\exp\left(-\int_0^{r}\left(1-\Pr^{\mathrm{L}}\left(\sqrt{u^2+(h_{\mathrm{UAV}}-h_{\mathrm{BS}})^2}\right)\right)2\pi u\lambda du\right)\\ *\left(1-\Pr_n^{\mathrm{L}}\left(\sqrt{r^2+(h_{\mathrm{UAV}}-h_{\mathrm{BS}})^2}\right)\right)2\pi r\lambda,\end{aligned} \tag{10}$$

where r_1 and r_2 are given implicitly by the following equations as

$$r_1=\arg_{r_1}\left\{\zeta^{\mathrm{NL}}\left(\sqrt{r_1^2+(h_{\mathrm{UAV}}-h_{\mathrm{BS}})^2}\right)=\zeta_n^{\mathrm{L}}\left(\sqrt{r^2+(h_{\mathrm{UAV}}-h_{\mathrm{BS}})^2}\right)\right\}, \tag{11}$$

and

$$r_2=\arg_{r_2}\left\{\zeta^{\mathrm{L}}\left(\sqrt{r_2^2+(h_{\mathrm{UAV}}-h_{\mathrm{BS}})^2}\right)=\zeta_n^{\mathrm{NL}}\left(\sqrt{r^2+(h_{\mathrm{UAV}}-h_{\mathrm{BS}})^2}\right)\right\}. \tag{12}$$

In addition, $\Pr\left[\frac{P\zeta_n^{\mathrm{L}}\left(\sqrt{r^2+(h_{\mathrm{UAV}}-h_{\mathrm{BS}})^2}\right)h}{I_{\mathrm{agg}}+N_0}>\gamma\right]$ and $\Pr\left[\frac{P\zeta_n^{\mathrm{NL}}\left(\sqrt{r^2+(h_{\mathrm{UAV}}-h_{\mathrm{BS}})^2}\right)h}{I_{\mathrm{agg}}+N_0}>\gamma\right]$ are respectively computed by

$$\Pr\left[\frac{P\zeta_n^{\mathrm{L}}\left(\sqrt{r^2+(h_{\mathrm{UAV}}-h_{\mathrm{BS}})^2}\right)h}{I_{\mathrm{agg}}+N_0}>\gamma\right]=\exp\left(-\frac{\gamma N_0}{P\zeta_n^{\mathrm{L}}\left(\sqrt{r^2+(h_{\mathrm{UAV}}-h_{\mathrm{BS}})^2}\right)}\right)\mathscr{L}_{I_{\mathrm{agg}}}^{\mathrm{L}}\left(\frac{\gamma}{P\zeta_n^{\mathrm{L}}\left(\sqrt{r^2+(h_{\mathrm{UAV}}-h_{\mathrm{BS}})^2}\right)}\right), \tag{13}$$

where $\mathscr{L}_{I_{\mathrm{agg}}}^{\mathrm{L}}(s)$ is the Laplace transform of I_{agg} for LoS signal transmission evaluated at s, which can be further written as

$$\begin{aligned}\mathscr{L}_{I_{\mathrm{agg}}}^{\mathrm{L}}(s)=\exp\left(-2\pi\tilde{\lambda}\int_r^{+\infty}\frac{\Pr^{\mathrm{L}}\left(\sqrt{u^2+(h_{\mathrm{UAV}}-h_{\mathrm{BS}})^2}\right)u}{1+\left(sP\zeta^{\mathrm{L}}\left(\sqrt{u^2+(h_{\mathrm{UAV}}-h_{\mathrm{BS}})^2}\right)\right)^{-1}}du\right)\\ *\exp\left(-2\pi\tilde{\lambda}\int_{r_1}^{+\infty}\frac{\left[1-\Pr^{\mathrm{L}}\left(\sqrt{u^2+(h_{\mathrm{UAV}}-h_{\mathrm{BS}})^2}\right)\right]u}{1+\left(sP\zeta^{\mathrm{NL}}\left(\sqrt{u^2+(h_{\mathrm{UAV}}-h_{\mathrm{BS}})^2}\right)\right)^{-1}}du\right),\end{aligned} \tag{14}$$

and

$$\Pr\left[\frac{P\zeta_n^{\mathrm{NL}}\left(\sqrt{r^2+(h_{\mathrm{UAV}}-h_{\mathrm{BS}})^2}\right)h}{I_{\mathrm{agg}}+N_0}>\gamma\right]=\exp\left(-\frac{\gamma N_0}{P\zeta_n^{\mathrm{NL}}\left(\sqrt{r^2+(h_{\mathrm{UAV}}-h_{\mathrm{BS}})^2}\right)}\right)\mathscr{L}_{I_{\mathrm{agg}}}^{\mathrm{NL}}\left(\frac{\gamma}{P\zeta_n^{\mathrm{NL}}\left(\sqrt{r^2+(h_{\mathrm{UAV}}-h_{\mathrm{BS}})^2}\right)}\right), \tag{15}$$

where $\mathscr{L}_{I_{\mathrm{agg}}}^{\mathrm{NL}}(s)$ is the Laplace transform of I_{agg} for NLoS signal transmission evaluated at s, which can be further written as

$$\begin{aligned}\mathscr{L}_{I_{\mathrm{agg}}}^{\mathrm{NL}}(s)=\exp\left(-2\pi\tilde{\lambda}\int_{r_2}^{+\infty}\frac{\Pr^{\mathrm{L}}\left(\sqrt{u^2+(h_{\mathrm{UAV}}-h_{\mathrm{BS}})^2}\right)u}{1+\left(sP\zeta^{\mathrm{L}}\left(\sqrt{u^2+(h_{\mathrm{UAV}}-h_{\mathrm{BS}})^2}\right)\right)^{-1}}du\right)\\ *\exp\left(-2\pi\tilde{\lambda}\int_{r}^{+\infty}\frac{\left[1-\Pr^{\mathrm{L}}\left(\sqrt{u^2+(h_{\mathrm{UAV}}-h_{\mathrm{BS}})^2}\right)\right]u}{1+\left(sP\zeta^{\mathrm{NL}}\left(\sqrt{u^2+(h_{\mathrm{UAV}}-h_{\mathrm{BS}})^2}\right)\right)^{-1}}du\right).\end{aligned} \tag{16}$$

Proof: We omit the proof due to page limitation. We will provide the full proof in the journal version of this paper. □

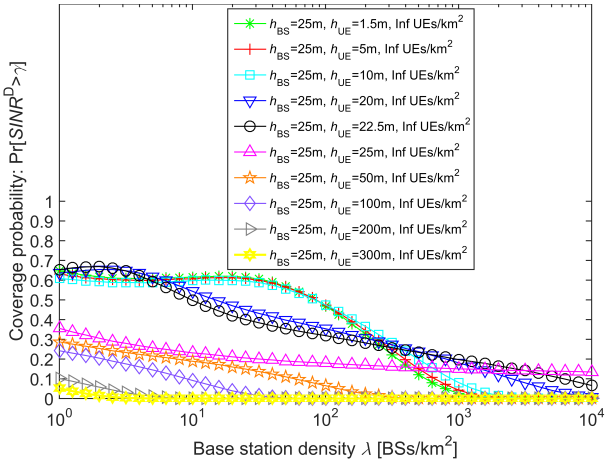

Fig. 2. $p^{\text{cov}}(\lambda, \gamma_0)$ vs. λ with $\gamma_0 = 0\,\text{dB}$, $\rho = +\infty$.

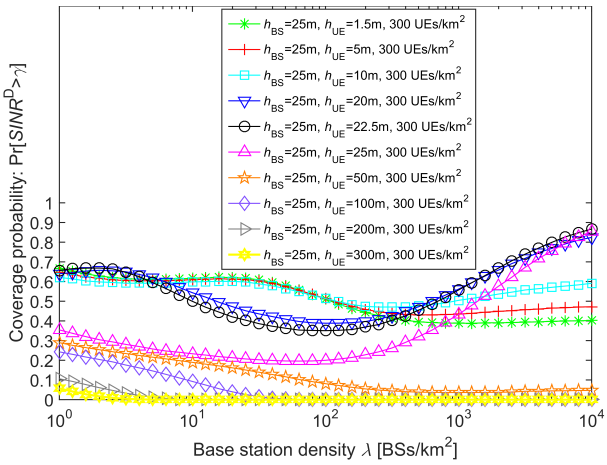

Fig. 3. $p^{\text{cov}}(\lambda, \gamma_0)$ vs. λ with $\gamma_0 = 0\,\text{dB}$, $\rho = 300\text{UEs/km}^2$.

$$\Pr^{\text{L}}(w) = \begin{cases} \Pr_1^{\text{L}}(w), & 1.5m \le h_{\text{UAV}} \le 22.5m \\ \Pr_2^{\text{L}}(w), & 22.5m < h_{\text{UAV}} \le 100m \\ 100\%, & 100m < h_{\text{UAV}} \le 300m \end{cases}. \tag{23}$$

$$\Pr_1^{\text{L}}(w) = \begin{cases} 100\%, & r \le 18m \\ (18/r + \exp(-r/63) * (1 - 18/r)) * & \\ (1 + (5/4)C' * (r/100)^3 * \exp(-r/150)) & r > 18m \end{cases}. \tag{24}$$

$$\text{C}' = \begin{cases} 0, & h_{\text{UAV}} \le 13m \\ [(h_{\text{UAV}} - 13)/10]^{1.5}, & 13m < h_{\text{UAV}} \le 23m \end{cases}, \tag{25}$$

$$\Pr_2^{\text{L}}(w) = \begin{cases} 100\%, & r \le d_1 \\ d_1/r + \exp(-r/p_1)(1 - d_1/r) & r > d_1 \end{cases}, \tag{26}$$

$$p_1 = 4300 \log_{10} h_{\text{UAV}} - 3800, \tag{27}$$

$$d_1 = \max(460 \log_{10} h_{\text{UAV}} - 700, 18). \tag{28}$$

where f_c is the centre frequency and is 2 GHz. The BS transmission power, P, is 46 dBm, and the UAV noise power, N_0, is -95 dBm.

A. Coverage Probability Analysis

In this section, we study the coverage probability. The BS antenna height is fixed to 25 m, and we vary the BS density as well as the UAV height. Fig. 2 shows results for an infinite UAV density, meaning that there is always one UAV to be served by each BS. Fig. 3 shows results for a finite UAV density, for which there may not always be a UAV to be served by each BS. In both figures, lines represent the results of the theoretical analysis and markers those of our simulations. From Fig. 2 and Fig. 3, we can observe the accuracy of our analytical framework, with a close match between theoretical and simulation results.

From these figures, we can make the following observations:

- When the UAV is higher than the BS, the coverage probability monotonically decreases to zero with the BS density. The larger the UAV height, the faster the coverage probability decreases towards zero. The trend is the same irrespective of whether the UAV density is infinite or finite. The reason for this overall behaviour is the ASE Crash. The larger the UAV height, the larger the probability of LoS, the antenna height difference between UAVs and BSs, as well as the cap on the signal power strength. Thus, the aggregated inter-cell interference power, although subject to the same cap, overwhelms the signal power in a denser network due to the large number of strong interferers.
- When the UAV is lower than the BS, the coverage probability is always larger than in the case when the UAV is higher than the BS. This is due to the ASE Crawl, i.e., the probability of LoS interference is much larger in the second case. This is true regardless of the UAV density.
- When the UAV density is infinite and the UAV is lower than the BS, we can observe that at low BS densities and for UAV heights up to 10 m, the coverage probability stays roughly constant. Two contradicting phenomena act here. The larger BS density enhances the signal power due to proximity, but it also brings the ASE Crawl, the transition of the strongest interferers from NLoS to LoS. Once the BS density is large enough, the ASE Crash kicks in, and the coverage probability goes to zero.
- When the UAV density is infinite and the UAV is lower than the BS but higher than 10 m, the ASE Crash kicks in quite early, and the coverage probability quickly goes to zero.
- When the UAV density is finite and the UAV is lower than the BS, the ASE Take Off appears at a BS density of around 100BS/km^2, enhancing the coverage probability, as some BSs are switched off since there are no UAVs in their coverage area.

B. Area Spectral Efficiency Analysis

In this section, we study the ASE. Similarly to the previous section, the BS antenna height is also fixed to 25 m, and we vary the BS density as well as the UAV height. Fig. 2 shows results for an infinite UAV density, when there is always one UAV to be served by each BS. Fig. 4 shows results for a finite

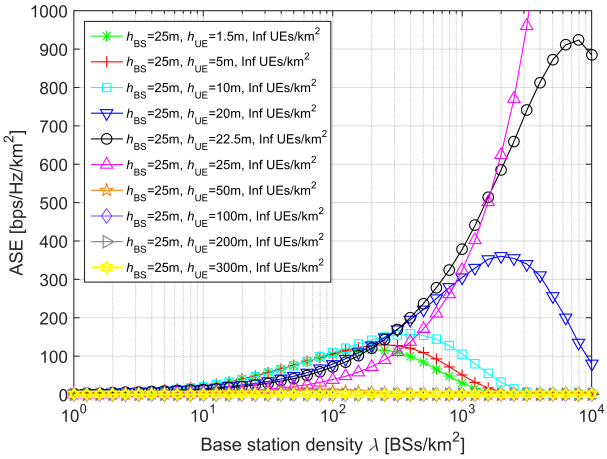

Fig. 4. $A^{\text{ASE}}(\lambda, \gamma_0)$ vs. λ with $\gamma_0 = 0\,\text{dB}$, $\rho = +\infty$.

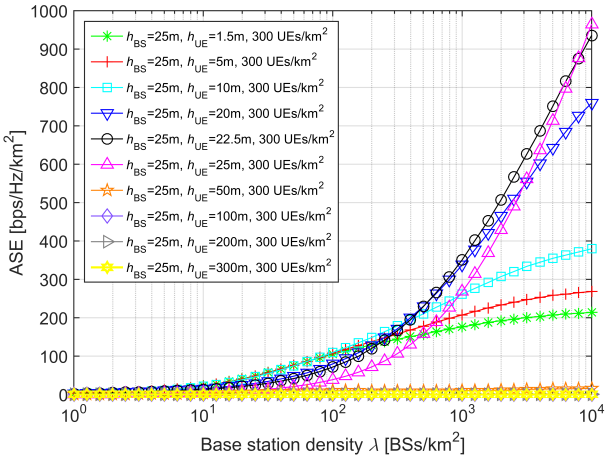

Fig. 5. $A^{\text{ASE}}(\lambda, \gamma_0)$ vs. λ with $\gamma_0 = 0\,\text{dB}$, $\rho = 300\text{UEs/km}^2$.

UAV density, implying that there may not always be a UAV to be served by each BS.

From these figures, we can extract the following conclusions:

- When the UAV is higher than the BS, the ASE is practically zero for all BS densities. The trend is the same no matter whether the UAV density is infinite or finite. The reason for this overall behaviour is the ASE Crash, and the resulting poor SINR, as explained in Section IV-A.
- When the UAV is lower than the BS, the ASE is always larger than the case when the UAV is higher than the BS. This is due to the ASE Crawl in the second case, and the resulting poorer SINR, as also explained in Section IV-A
- When the UAV density is infinite and the UAV is lower than the BS, we can see that the ASE first increases with the BS density, as there is a better spatial reuse, but then decreases due to ASE Crash. The closer the UAV height is to the BS height, the latter the ASE Crash kicks in. When UAV and BS are at the same height, the ASE Crash is completely removed, and the ASE monotonically grows with the BS density.
- When the UAV density is finite and the UAV is lower than the BS, the ASE Take Off appears at a BS density of around 100 BS/km^2, significantly enhancing the ASE, because of the surplus of BS and the idle mode capability, which switches off BSs with no UAVs, with the resulting interference mitigation.
- When looking to the ASE, two regimes can be found. At low and medium BS densities, e.g., $<$500 BS/km^2, it is better to fly the drones low, at a height of around 10 m. This is to reduce LoS interference. At high BS densities, e.g., $>$500 BS/km^2, it is better to fly the drones at around the BS height of 25 m. This is to avoid the ASE Crash.

V. Conclusion

In this paper, we have provided a theoretical analysis of the DL command and control channel performance using the comprehensive path loss model recommended by the 3GPP in [11] with LoS and NLoS transmissions and a probabilistic, UAV height dependent model, to switch between them. We have also derived theoretical expressions for the coverage probability and ASE, while accounting for BSs with idle mode capabilities, a finite UAV density, different UAV heights and different levels of densification. From this analysis, one can observe that cellular networks with omnidirectional BS antennas can provide a reasonable coverage for low-height UAVs, flying at heights close to those of the BSs, where network densification can bring significant benefits. For high height UAVs, inter-cell interference coordination measures are needed, as the ASE is poor, and the command and control channel cannot be provided with high reliability.

References

[1] New America, "Drones and aerial observation: New technologies for property rights, human rights, and global development – A primer," July 2015.

[2] M. Mozaffari, W. Saad, M. Bennis, Y.-H. Nam, and M. Debbah, "A tutorial on UAVs for wireless networks: Applications, challenges, and open problems," available as *arXiv:1803.00680,* Mar. 2018.

[3] Y. Zeng, J. Lyu, and R. Zhang, "Cellular-connected UAV: Potentials, challenges and promising technologies," available as *arXiv:1804.02217,* Apr. 2018.

[4] Y. Zeng, R. Zhang, and T. J. Lim, "Wireless communications with unmanned aerial vehicles: Opportunities and challenges," *IEEE Commun. Mag.*, vol. 54, no. 5, pp. 36–42, May 2016.

[5] H. C. Nguyen, R. Amorim, J. Wigard, I. Z. Kovács, T. B. Sørensen, and P. E. Mogensen, "How to Ensure Reliable Connectivity for Aerial Vehicles Over Cellular Networks," *IEEE Access*, vol. 6, pp. 12 304–12 317, 2018.

[6] B. van der Bergh, A. Chiumento, and S. Pollin, "LTE in the sky: Trading off propagation benefits with interference costs for aerial nodes," *IEEE Commun. Mag.*, vol. 54, no. 5, pp. 44–50, May 2016.

[7] S. Hayat, E. Yanmaz, and R. Muzaffar, "Survey on unmanned aerial vehicle networks for civil applications: A communications viewpoint," *IEEE Commun. Surveys and Tutorials*, vol. 18, no. 4, pp. 2624–2661, Fourth Quarter 2016.

[8] V. Yajnanarayana, Y.-P. E. Wang, S. Gao, S. Muruganathan, and X. Lin, "Interference mitigation methods for unmanned aerial vehicles served by cellular networks," available as *arXiv:1802.00223,* Feb. 2018.

[9] M. M. Azari, F. Rosas, and S. Pollin, "Reshaping cellular networks for the sky: The major factors and feasibility," available as *arXiv:1710.11404,* Oct. 2017.

[10] X. Lin, V. Yajnanarayana, S. D. Muruganathan, S. Gao, H. Asplund, H. L. Maattanen, M. Bergström, S. Euler, and Y.-P. E. Wang, "The sky is not the limit: LTE for unmanned aerial vehicles," *IEEE Commun. Mag.*, vol. 56, no. 4, pp. 204–210, Apr. 2018.

[11] 3GPP Technical Report 36.777, "Technical specification group radio access network; Study on enhanced LTE support for aerial vehicles (Release 15)," Dec. 2017.

[12] G. Geraci, A. Garcia Rodriguez, L. Galati Giordano, D. López-Pérez, and E. Björnson, "Understanding UAV cellular communications: From existing networks to massive MIMO," available as *arXiv:1804.08489,* Apr. 2018.

[13] ——, "Supporting UAV cellular communications through massive MIMO," in *Proc. IEEE ICC Workshops,* May 2018, to appear. Available as *arXiv:1802.01527*.

[14] W. Khawaja, I. Guvenc, D. W. Matolak, U.-C. Fiebig, and N. Schneckenberger, "A survey of air-to-ground propagation channel modeling for unmanned aerial vehicles," available as *arXiv:1801.01656,* Jan. 2018.

[15] M. Ding, P. Wang, D. López-Pérez, G. Mao, and Z. Lin, "Performance Impact of LoS and NLoS Transmissions in Dense Cellular Networks," *IEEE Trans. Wireless Commun.*, vol. 15, no. 3, pp. 2365–2380, Mar. 2016.

[16] M. Ding and D. López-Pérez, "Performance Impact of Base Station Antenna Heights in Dense Cellular Networks," *IEEE Trans. Wireless Commun.*, vol. 16, no. 12, pp. 8147–8161, Dec. 2017.

[17] M. Ding, D. López-Pérez, G. Mao, and Z. Lin, "Performance Impact of Idle Mode Capability on Dense Small Cell Networks," *IEEE Trans. Veh. Technol.*, vol. 66, no. 11, pp. 10 446–10 460, Nov. 2017.

[18] M. Ding, D. López-Pérez, and G. Mao, "A new capacity scaling law in ultra-dense networks," available as *arXiv:1704.00399,* Apr. 2017.

[19] S. Lee and K. Huang, "Coverage and economy of cellular networks with many base stations," *IEEE Commun. Letters*, vol. 16, no. 7, pp. 1038–1040, Jul. 2012.

[20] M. Ding, D. López-Pérez, G. Mao, and Z. Lin, "Study on the idle mode capability with LoS and NLoS transmissions," in *Proc. IEEE Globecom*, Dec. 2016, pp. 1–6.

[21] T. Bai and R. Heath, "Coverage and rate analysis for millimeter-wave cellular networks," *IEEE Trans. Wireless Commun.*, vol. 14, no. 2, pp. 1100–1114, Feb. 2015.

[22] X. Zhang and J. Andrews, "Downlink cellular network analysis with multi-slope path loss models," *IEEE Trans. Commun.*, vol. 63, no. 5, pp. 1881–1894, May 2015.

[23] M. Ding, D. López-Pérez, G. Mao, P. Wang, and Z. Lin, "Will the area spectral efficiency monotonically grow as small cells go dense?" in *Proc. IEEE Globecom*, San Diego, CA, USA, Dec. 2015, pp. 1–7.